The Kohn-Sham density of states and band gap of water: From small clusters to liquid water

P. Cabral do Couto, S. G. Estácio, and B. J. Costa Cabral[a)]
Departamento de Química e Bioquímica, Faculdade de Ciências, Universidade de Lisboa, 1749-016 Lisboa, Portugal and Grupo de Fýsica Matemýtica da Universidade de Lisboa, Avenida Professor Gama Pinto 2, 1649-003 Lisboa, Portugal

(Received 27 April 2005; accepted 1 June 2005; published online 9 August 2005)

Electronic properties of water clusters $(H_2O)_n$, with $n=2$, 4, 8, 10, 15, 20, and 30 molecules were investigated by sequential Monte Carlo/density-functional theory (DFT) calculations. DFT calculations were carried out over uncorrelated configurations generated by Monte Carlo simulations of liquid water with a reparametrized exchange-correlation functional that reproduces the experimental information on the electronic properties (first ionization energy and highest occupied molecular orbital-lowest unoccupied molecular orbital gap) of the water dimer. The dependence of electronic properties on the cluster size (n) shows that the density of states (DOS) of small water clusters $(n>10)$ exhibits the same basic features that are typical of larger aggregates, such as the mixing of the $3a_1$ and $1b_1$ valence bands. When long-ranged polarization effects are taken into account by the introduction of embedding charges, the DOS associated with $3a_1$ orbitals is significantly enhanced. In agreement with valence-band photoelectron spectra of liquid water, the $1b_1$, $3a_1$, and $1b_2$ electron binding energies in water aggregates are redshifted by ~ 1 eV relative to the isolated molecule. By extrapolating the results for larger clusters the threshold energy for photoelectron emission is 9.6 ± 0.15 eV (free clusters) and 10.58 ± 0.10 eV (embedded clusters). Our results for the electron affinity ($V_0=-0.17\pm0.05$ eV) and adiabatic band gap ($E_{G,\mathrm{Ad}}=6.83\pm0.05$ eV) of liquid water are in excellent agreement with recent information from theoretical and experimental works. © *2005 American Institute of Physics*. [DOI: 10.1063/1.1979487]

I. INTRODUCTION

Water is the most important liquid for life and chemical reactivity in liquid water is a fundamental process characterizing the behavior of many living organisms. Therefore, the structure, energetics, and electronic properties of liquid water were the subject of numerous investigations.[1–7] Some properties of liquid water are unique, fascinating, and worth referring: the structure of water is characterized by a complex hydrogen (H)-bond network which leads to a very specific dependence of the density on the thermodynamic state and to the water density anomaly at $T=4\ ^\circ\mathrm{C}$;[8] the strong polarizability of liquid water, which is related to cooperative effects induced by H bonding, determines its dielectric properties as well as the significant increase of the water molecule dipole moment from 1.85 D in the gas to ~ 2.6 D in the liquid phase.[9,10] In comparison with its energetics and structure, the electronic properties of liquid water[3,11–22] are apparently not well understood. One specific aspect concerns the band gap of water.[3,11,14,16,17,19,20] It is generally accepted that water can be described as a very large band-gap amorphous semiconductor.[11,17] However, it is not obvious that the band gap of liquid water can be uniquely associated with an optical (vertical) excitation process, where the gap is defined simply as the highest occupied molecular orbital-lowest unoccupied molecular orbital (HOMO-LUMO) energy difference. As recently pointed out by Coe *et al.*,[3] the reactive nature of electronically excited water molecules,[18] the reorganization of water molecules around charged species in liquid phase, and the observed photophysics of anionic defects (known as the anion problem)[4] strongly indicate that an adiabatic route can be defined for accessing the conduction-band edge in liquid phase. Moreover, given that the time scale of the solvent relaxation is much larger than the vertical process, the adiabatic band gap of liquid water cannot be determined vertically.

From the theoretical point of view, electronic properties of liquid water were the subject of several studies.[3,23–26] It is well known that *ab initio* molecular dynamics (ABMD) simulations are of great interest for investigating the electronic properties in condensed phase. Although the complexity of liquid water makes a first-principles approach rather difficult, several ABMD simulations were carried out[27–34] and some of them also reported results for the HOMO-LUMO gap and the density of states (DOS).[27,32,33] However, only few works on the adiabatic band gap of liquid water were reported.[3,4] Another aspect of interest concerns the relationship between H bonding and the electronic properties of water.[35–40] In this sense, specific issues including the size dependence of the electronic properties, the influence of surface effects on the DOS, and water band gap certainly deserve further attention.

The present article is focused on the electronic properties of water, in particular, on its density of states (DOS),

[a)]Author to whom correspondence should be addressed. Electronic mail: ben@adonis.cii.fc.ul.pt

HOMO-LUMO gap (E_G), and adiabatic band gap ($E_{G,\mathrm{Ad}}$). A sequential Monte Carlo/quantum mechanics approach[41,42] was adopted. From uncorrelated supermolecular structures generated by Monte Carlo simulations for liquid water, density-functional theory (DFT) calculations were carried out to study the electronic properties of water aggregates of different sizes. Surface effects were then minimized and long-ranged electrostatic interactions were taken into account by the introduction of embedding charges, as an approximation to the liquid environment.

DFT calculations were carried out with a reparametrization of the Adamo and Barone modified exchange-correlation functional (MPW1PW91).[43–45] The reparametrized functional reproduces experimental information on the electronic properties of the water dimer. The article is organized as follows. Initially, we describe the generation of the aggregates by the Monte Carlo method and the reparametrization of the MPW1PW91 functional. A detailed analysis of size dependence and surface effects is then reported. Finally, extrapolated results for larger water aggregates (free and embedded in a charge distribution) are reported and compared with experimental information and theoretical predictions for liquid water from other studies. We conclude by placing emphasis on the difference between the optical and the adiabatic band gap of liquid water.

II. COMPUTATIONAL DETAILS

A. Monte Carlo simulations

The interactions between water molecules were described by the TIP5P potential.[46] This model, which has been designed to reproduce the water density anomaly at $T=4\ ^\circ\mathrm{C}$,[46] predicts the structural and thermodynamic properties of liquid water in excellent agreement with experiment. The TIP5P charge distribution is described by two negatively charged ($-0.241\ e$) sites located symmetrically along the lone pair directions and a positive charge ($+0.241\ e$) on each hydrogen site.[46] It is important to observe that this model predicts a dielectric constant of water ($\epsilon=81.5\pm1.5$) in very good agreement with experiment ($\epsilon=79.3$). Monte Carlo (MC) simulations of water were carried out in the isobaric-isothermal (npT) ensemble[47] at $T=298$ K and $p=1$ atm in a cubic box with periodic boundary conditions. The number of water molecules is $n=500$ and the interactions are truncated at a cutoff radius of 9.0 Å. We carried out 10^8 MC steps for equilibration. This run was followed by 1.25×10^9 additional MC steps. Each step involves the attempt to move one molecule of the system. From the configurations generated by the MC procedure $N=50$ uncorrelated configurations were selected by determining a correlation time over the MC Markov chain.[41,42] We note that successive configurations generated by the Metropolis algorithm[48] are strongly correlated. When the property of interest involves a high computational effort, the use of uncorrelated structures is of crucial importance for evaluating the averages over a relatively small number of representative configurations.[41,42]

Each uncorrelated configuration corresponds to a supermolecular structure (water cluster) including explicitely n molecules. The structure of the clusters corresponds to the liquid-phase structure at $T=298$ K and no geometry optimization of the aggregates was carried out. Size dependence was investigated by carrying out calculations with $n=1$, 2, 4, 8, 10, 15, 20, 30. Surface effects and long-ranged corrections to polarization effects were investigated by embedding the clusters in the TIP5P charge distribution of the surrounding water molecules. Thus, no periodic boundary conditions were applied for evaluating the electronic properties. The number of embedding water molecules is represented by n_c. We have taken $n_c=200$. Some calculations based on the Kirkwood-Onsager model,[49] where the clusters are placed in a spherical cavity surrounded by a continuum dielectric medium, were also carried out.

B. Density-functional theory calculations

The electronic properties of the clusters were determined by performing DFT calculations over uncorrelated MC configurations. Although the physical meaning of Kohn-Sham (KS) orbital energies remains a controversial issue in the literature,[50,51] several works provided evidence that DFT can correctly predict electron binding energies.[52–61] The disagreement between KS electron binding energies predicted by the widely used exchange-correlation functionals and experiment is related to the self-interaction error in DFT.[62] An interesting possibility is to parametrize the exchange-correlation functional for reproducing experimental electron binding energies.[53,57] The present approach to study the electronic properties of water is based on the following semiempirical procedure. The modified Perdew-Wang functional (MPW1PW91) proposed by Adamo and Barone[43–45] has been reparametrized to reproduce the electronic properties of the water dimer. The reparametrization was based on the representation of the exchange-correlation functional as[43–45]

$$E_{\mathrm{xc}}=(1-\alpha)E_x^{\mathrm{HF}}+\alpha(E_x^{\mathrm{Slater}}+\Delta E_x^{\mathrm{mPW}})+E_c^{\mathrm{local}}+\Delta E_c^{\mathrm{PW91}}, \tag{1}$$

where $\Delta E_{\mathrm{x}}^{\mathrm{mPW}}$ is the modified Perdew-Wang exchange-correlation functional, and E_c^{local} is the local correlation functional contribution.

We have determined the optimal value of α in the above expression that reproduces the first ionization potential of the water dimer (11.21 ± 0.09 eV).[63] DFT calculations were carried out with Woon and Dunning's correlation consistent polarized valence double zeta basis set augmented with diffuse functions (aug-cc-pVDZ).[64] We find that the optimal value of α is 0.375. The MPW1PW91 standard value is $\alpha=0.75$. The results for several properties of the water dimer predicted by the present reparametrization are reported in Table I, where they are compared with experimental data and theoretical results based on Hartree-Fock (HF) calculations, coupled cluster with single and double excitations and perturbative inclusion of triples [CCSD(T)],[65–68] and Møller-Pleset perturbation theory[69] at fourth order (MP4). CCSD(T) and MP4 results for the vertical attachment energies (VAE) and electron binding energies were based on ΔE calculations.

Table I reports (see values in brackets) the electron binding energies relative to the HOMO. For the valence orbitals, these differences are roughly the same for HF calculations

TABLE I. Theoretical and experimental results for the water dimer $(H_2O)_2$. The distances are in angstroms. The binding energies (ΔE_b) are in kJ mol^{-1}. The dipole moments (μ) are in debye. The vertical attachment energies (VAE), HOMO-LUMO energy differences (E_G), and electron binding energies are in eV. The frequencies are in cm^{-1}. For the dimer, [a] and [d] denote the role played (as proton acceptor or donor) by the water molecule for which the contribution from a given orbital is dominant. The numbers in brackets are electron binding energies relative to the HOMO. The calculations were performed with the aug-cc-pVDZ basis set.

		MPW1PW91				
	HF	α=0.750[a]	α=0.375[b]	CCSD(T)	MP4	Expt.
d(O–O)	3.032	2.892	2.864	2.926	2.917	2.976±0.03[c]
ΔE_b	−16.40	−20.1	−21.8	−22.2	−22.5	−20.9±0.5[d]
μ	2.9	2.6	2.7	2.7	2.7	2.6[e]
VAE	-0.80	0.73	-0.13	0.49	0.50	0.050±0.03[f]
E_G	13.97	7.65	11.33	12.48	12.57	11.16±0.05[g]
$1b_1$ [d]	13.15	8.38	11.20	12.97	13.07	11.21±0.09[h]
$(3a_1,1b_1)$ [a]	14.48[1.3]	9.76[1.4]	12.60[1.4]			
$(3a_1,1b_1)$ [d]	15.12[2.0]	10.51[2.1]	13.34[2.1]			
$3a_1$ [a]	16.67[3.5]	12.05[3.7]	14.91[3.7]			
$1b_2$ [d]	19.22[6.1]	14.36[6.0]	17.34[6.1]			
$1b_2$ [a]	20.47[7.3]	15.75[7.4]	18.72[7.5]			
$2a_1$ [d]	36.34[23.2]	27.68[19.3]	32.53[21.3]			
$2a_1$ [a]	37.72[24.6]	29.28[20.9]	34.15[23.0]			
O($1s$) [d]	559.09[545.9]	522.89[514.5]	541.14(540.20)[i][529.9]			
O($1s$) [a]	560.46[547.3]	524.47[516.1]	542.74(541.48)[i][530.2]			
ν_1		3957	4171			3745[j]
ν_2		3936	4152			3730[j]
ν_3		3849	4062			3600[j]
ν_4		3720	3951			3539[j]
ν_5		1651	1716			1619[j]
ν_6		1629	1693			1601[j]

[a]MPW1PW91 parametrization (Refs. 43–45).
[b]Present parametrization.
[c]From Odutola and Dyke (Ref. 71).
[d]From Feyerisen *et al.* (Ref. 72).
[e]From Dyke *et al.* (Ref. 73).
[f]From Kim *et al.* (Ref. 74).
[g]Estimated from the experimental ionization potential (IP) and vertical attachment energy (VAE) as IP-VAE.
[h]From Ng *et al.* (Ref. 63).
[i]Theoretical results based on CASSCF/aug-cc-pVDZ calculations. From Felicissimo *et al.* (Ref. 70).
[j]From Huang and Miller (Ref. 75).

and for the two MPW1PW91 parametrizations. In a comparative analysis of HF and KS energies, Politzer and Abu-Awwad[54] pointed out that, for a given molecule, different exchange-correlation functionals lead to KS valence orbital energies, which differ from experimental data nearly by a constant value. The present results confirm this behavior. Moreover, they indicate that when the functional is parametrized to reproduce the HOMO energy, the whole set of orbital energies is in good agreement with experiment. For example, our results for the water dimer O($1s$) binding energies (541.14 and 542.74 eV) are very close to theoretical predictions based on complete active space self-consistent field (CASSCF) calculations (540.2 and 541.1 eV).[70] This agreement leads credence to our parametrization for reproducing the core DOS of water aggregates, although our main interest is focused on the valence binding energies and HOMO-LUMO gap.

Although the present reparametrization was oriented to reproduce the first ionization potential, several properties of the water dimer, including the structure,[71] binding energy,[72] dipole moment,[73] vertical attachment energy (VAE),[74] and HOMO-LUMO gap (E_G), are in excellent agreement with experiment and other theoretical approaches. As expected, unscaled harmonic vibrational frequencies are slightly overestimated in comparison with experimental values.[75] We interpret the agreement between our predictions and experimental information for several properties of the water dimer as a strong indication on the reliability of the present approach for investigating the electronic properties of water clusters. The quantum-mechanical calculations were carried out with the GAUSSIAN-98 program.[76]

III. THE ELECTRONIC DENSITY OF STATES IN WATER CLUSTERS

A. Size dependence of electronic properties in free water clusters

The KS orbitals for the optimized structures of the water monomer (w_1), dimer (w_2), and tetramer (w_4) are illustrated in Fig. 1. For the monomer (w_1) they correspond to the $4a_1$, $1b_1$, $3a_1$, and $1b_2$ orbitals. (The $2a_1$ orbital at −33.4 eV is not shown.) $1b_1$ is the highest occupied molecular orbital

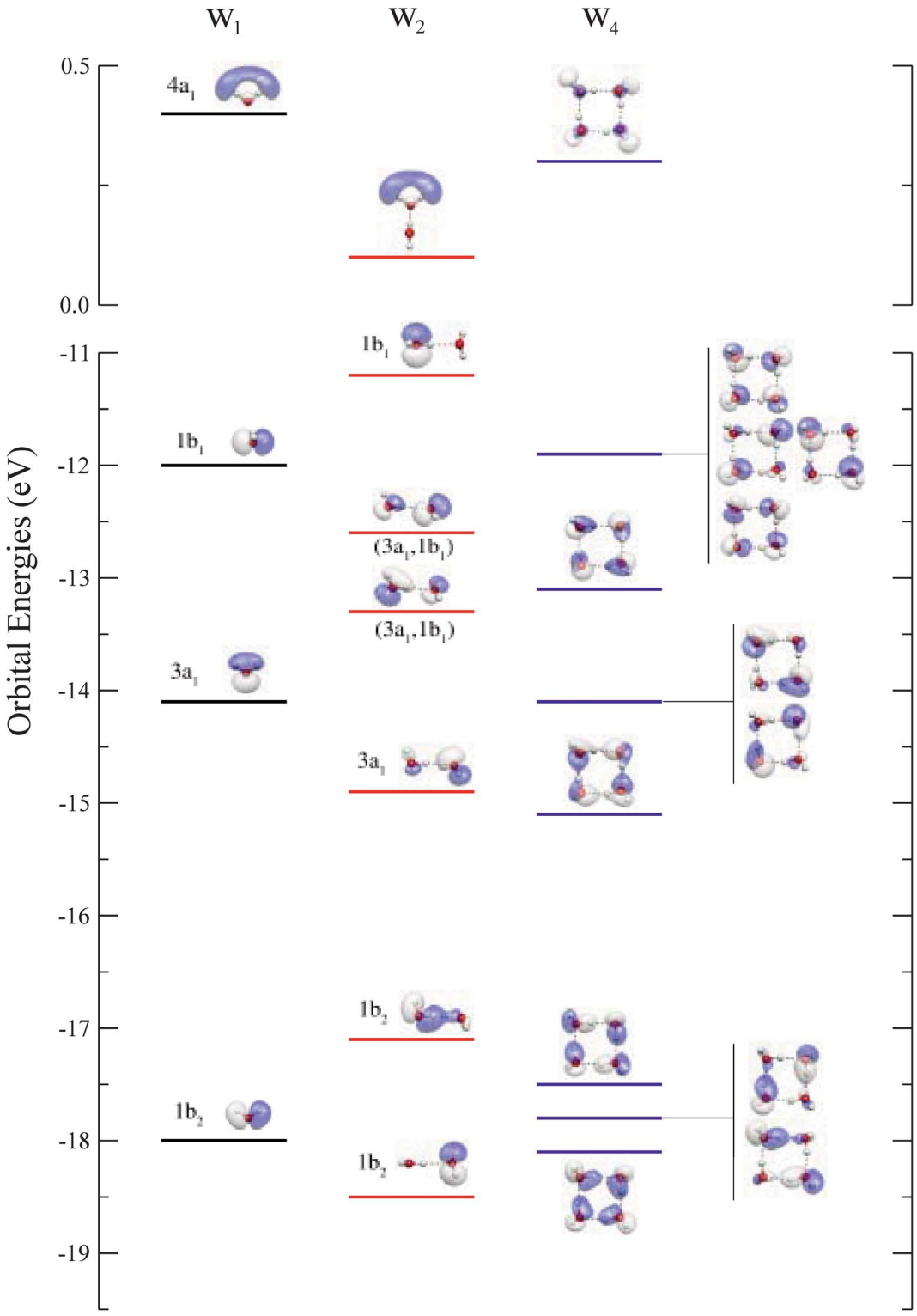

FIG. 1. (Color) Orbital energies (in eV) for the optimized gas-phase structures of the water monomer (w_1), dimer (w_2), and tetramer (w_4).

(HOMO) at the top of the water molecule "valence band." The $1b_1$ orbital has a strong $2p$ character and is centered at the site of the O($1s$) core orbital. For the water dimer (w_2) the HOMO corresponds essentially to the $1b_1$ orbital. The next two lower orbitals involve overlap between $3a_1$ and $1b_1$ orbitals and are represented in Fig. 1 as $(3a_1, 1b_1)$. The next-lowest dimer orbital is essentially a $3a_1$ orbital centered at the proton accepting water molecule. The two lowest occupied orbitals of w_2, represented in Fig. 1, are dominated by the contributions from $1b_2$, although the higher one involves some overlap with the $3a_1$ orbital. The most stable $1b_2$ orbital of the dimer correspond essentially to the energetically stabilized monomer orbital upon dimer formation. The splitting of the monomer orbital energies upon dimer formation reflects the feature that each water molecule plays a different role (as a proton donor or proton acceptor). The degeneracy

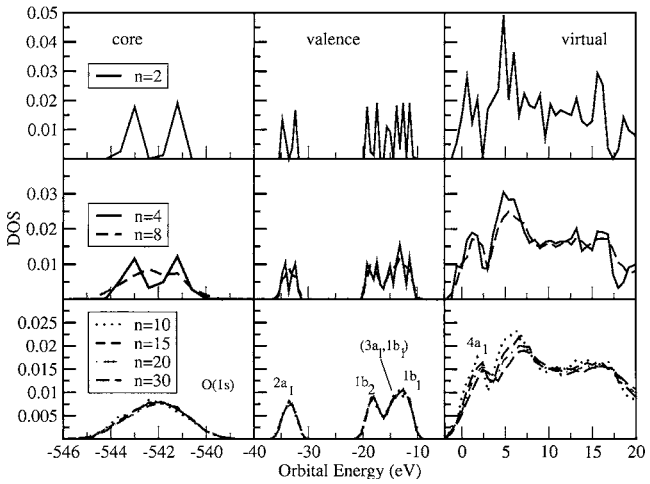

FIG. 2. Dependence of the average density of states (DOS) on the number of water molecules in the cluster (n=2, 4, 8, 10, 15, 20, 30) for free water clusters. MPW1PW91[α=0.375]/aug-cc-pVDZ results. Averages were carried out over 50 uncorrelated MC configurations.

of electron binding energies of the water tetramer (w_4) reflects its symmetrical cyclic structure. The highest occupied orbitals involve the $1b_1$ and $3a_1$ interactions and are related to the orbitals of the water dimer. We stress the specific role played by the $3a_1$ orbital in H bonding. As indicated in Fig. 1, H bonding involves mixing of $3a_1$ and $1b_1$ orbitals. This feature will induce broadening of the $3a_1$ and $1b_1$ bands upon condensation.[37] Also represented in Fig. 1 is the virtual $4a_1$ orbital (LUMO), which plays a central role in the energetic stabilization of an excess electron through the formation of a dipole-bound anion structure.[77,78] The energetical stabilization of the dimer $4a_1$ orbital relative to the monomer illustrates the stabilization of the LUMO (or the increase of the electronic affinity) upon dimer formation. The structure and orbital energies of small water clusters are the departure points to discuss the density of states (DOS) of larger clusters, and the characterization of their respective bands, which will keep a close relationship with the distribution of orbital energies of the small aggregates.

The size dependence of the density of states (DOS) is illustrated in Fig. 2, where the average DOS for water clusters of different sizes is reported. These clusters are supermolecular uncorrelated structures generated by the MC simulations of liquid water. We note that in the case of w_2 and w_4 they do not necessarily correspond to the gas-phase optimized structures of Fig. 1, because the structure of the aggregates taken from the simulations reflects the thermal fluctuations in the liquid phase. Therefore, the DOS of the uncorrelated structures will reflect thermal as well as electronic broadening.[33] The latter effect is basically related to the interactions between the water molecules. On the other hand, thermal fluctuations will be associated with the presence of different configurations at a finite temperature T.

The average DOS for the w_2 cluster associated with the $1b_2$ orbital is bimodal. Their peaks correspond roughly to the orbital energies of Fig. 1. For larger clusters the DOS becomes a broad distribution due to the presence of an increasing number of nearly isoenergetic isomers (thermal broadening). A similar pattern (from peaked to broad DOS) is observed in the formation of the $3a_1$ and $1b_1$ bands. For larger clusters ($n>10$) the $3a_1$ and $1b_1$ bands overlap appearing as a single distribution due to thermal and electronic broadening. The results shown in Fig. 2 indicate that the average DOS of small water aggregates is not dependent on the number of water molecules for $n>15$. The behavior of the core DOS with the cluster size reflects the expected dispersion of the core energies related to different structures and shows that the maxima position of the DOS is not changed for $n>10$.

The DOS of unoccupied orbitals is characterized by two peaks related to the $4a_1$ and $2b_1$ orbitals. For larger clusters ($n>10$) a shoulder (or preedge feature) near the bottom of the conduction band and a broad distribution centered at $\sim$10 eV are observed. Recent x-ray absorption spectroscopy (XAS) experiments[36] provided evidence on significant differences between the XAS spectra of ice and water in liquid and gaseous phases. These differences were related to structural features of the H-bond network and the spectra exhibit a strong dependence of the H-bonding environment.[36,39] Specifically, the presence of a preedge feature at the bottom of the conduction band was associated with broken H bonds. Therefore, a strong preedge is typical of small water clusters where free hydrogen atoms can act as H-bond acceptors. In contrast, only a weak structure is observed in ice, which is an indication of a fully coordinated H-bond network.[36] The behavior of the conduction-band DOS with the cluster size (Fig. 2) shows that the preedge feature is reduced with increasing n, which is an indication of H-bond formation. Moreover, the second broad peak at the high-energy range increases with the cluster size. These findings are in keeping with experimental[36] and theoretical studies[36,39] on x-ray absorption in water and water clusters.

The top of the valence band is related to the nonbonding orbital $1b_1$ (HOMO) and the difference between the HOMO and the bottom of the conduction band (or the average value of the LUMO) defines the optical band gap (E_G). The average energy of the LUMO for a cluster with n water molecules can be associated with the average electron affinity of the aggregates and it is represented as $V_{0,n}$.

The convergence of the DOS or the averaged orbital energies with the number of uncorrelated supermolecular structures (N) is illustrated in Fig. 3, where the cumulative average energies of the LUMO (top) and HOMO (bottom) as a function of N, for clusters of different size (n), are represented. In agreement with previous investigations of the dipole moment of liquid water based on sequential Monte Carlo/quantum mechanics calculations,[10] we observe that N =50 uncorrelated configurations are adequate for a reliable prediction of converged average properties.

Average HOMO energies are redshifted with increasing n. They change from $\sim$−11 (n=2) to $\sim$−9.6 eV (n=30). The dependence of the LUMO energy on the cluster size is also illustrated in Fig. 3. The LUMO energy is shifted to lower energies as the cluster size increases. From the water monomer to the cluster with n=30, the LUMO energy is stabilized by $\sim$1 eV. This tendency may be related to the formation of local structures involving the simultaneous presence of a number of free or dangling hydrogen atoms,

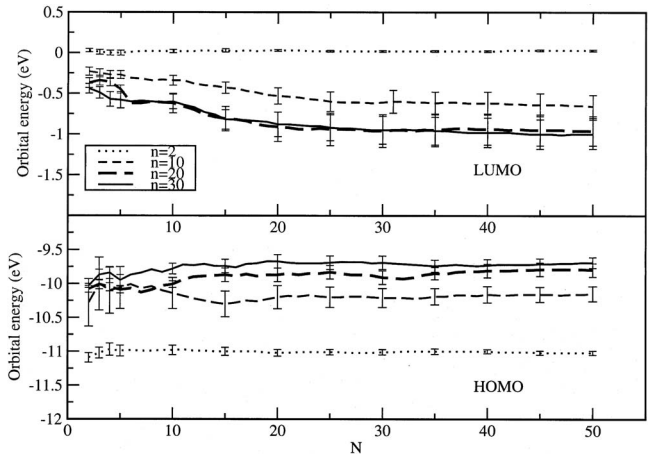

FIG. 3. Dependence of the average HOMO and LUMO energies on the number of uncorrelated configurations (N) for free water clusters of different size n.

mainly at the cluster surface. This number should increase with n because it depends on the number of water molecules close to the surface. Therefore, it seems reasonable to observe that the stabilization of the LUMO or the increase of the clusters electronic affinity with n can be related to surface effects.

B. Introduction of embedding charges: Influence on the water density of states

The uncorrelated supermolecular structures generated by the Monte Carlo simulations are water clusters, where surface effects are certainly significant. Although the calculations for free water clusters indicate the possibility to extrapolate the results for larger clusters, it is of interest to discuss how long-ranged polarization effects can be included and how surface effects can be minimized. Consequently, we have adopted the same strategy used for predicting the average dipole moment of the water molecule in liquid water.[10] Let us consider the larger aggregate ($n=30$). To this supermolecular structure, which has been selected from uncorrelated Monte Carlo simulations with 500 water molecules, the nonpolarizable TIP5P charge distribution of $n_c=200$ surrounding water molecules were added.

We should expect that the introduction of charge distribution mainly affects the water molecules closer to the cluster surface. To illustrate this effect we have calculated the difference of the electronic density in free and embedded clusters. Electronic density differences were calculated with the MOLEKEL visualization package[79] and isosurfaces representing these quantities are shown in Fig. 4. The main changes of the electronic density concern the water molecules close to the surface. No significant changes are observed in the electronic density of the inner molecules. Figure 5 shows the DOS for the free and embedded $\dot{w}_{30}$ aggregates. The core DOS is only slightly modified by the presence of the charges, which lead to a narrower peak centered at ~ -542 eV. This reflects a more homogeneous distribution of the electronic states in the embedded clusters and involves mainly the stabilization of core states for the water molecules close to the charge distribution.

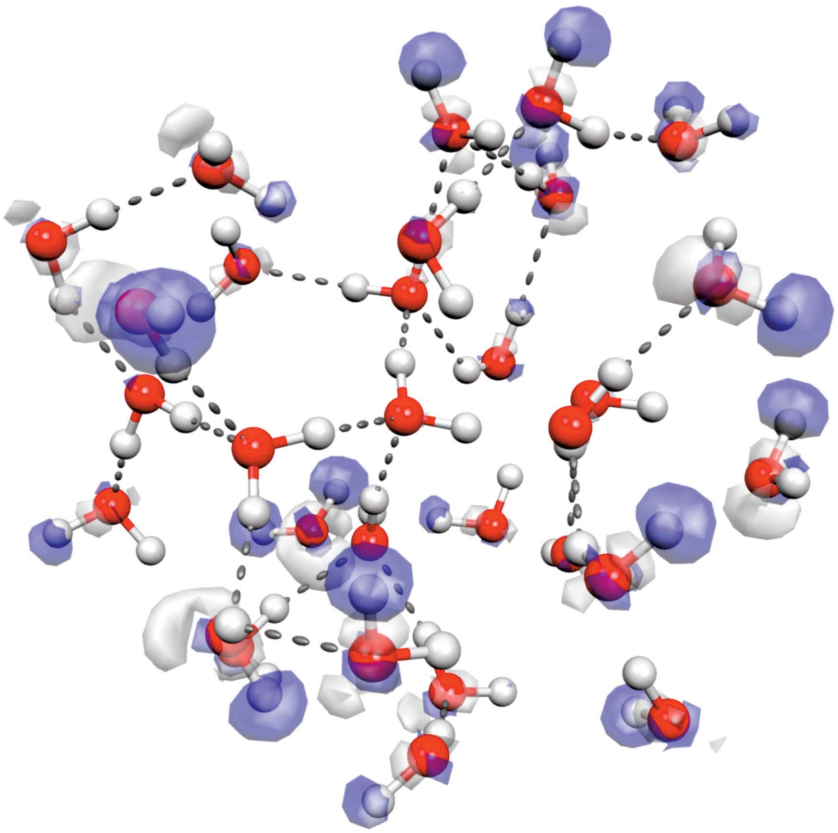

FIG. 4. (Color) Isosurfaces corresponding to the electronic density difference between free and embedded water clusters with $n=30$. The isosurfaces correspond to electronic density differences of -0.0025 (dark) and 0.0025 e Å^{-3} (white). The number of surrounding water molecules (represented by TIP5P charges) is $n_c=200$.

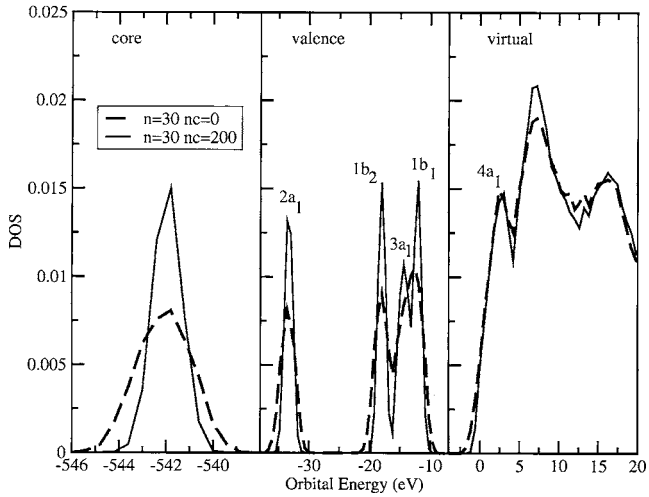

FIG. 5. Dependence of the DOS on the introduction of embedding charges (n_c=200). Results for the w_{30} cluster.

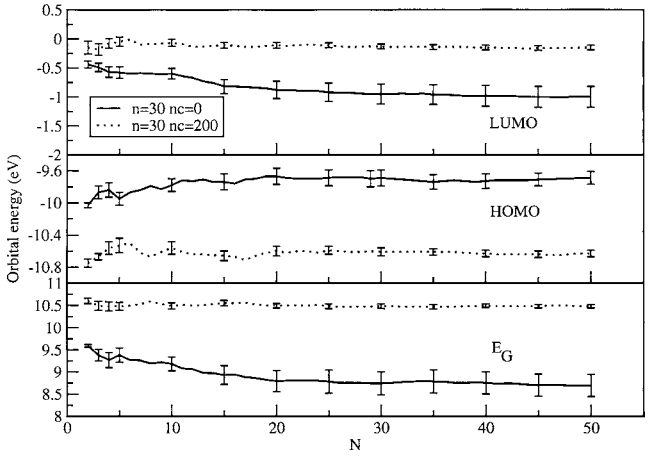

FIG. 6. Dependence of the HOMO and LUMO energies, and optical band gap E_G on the introduction of embedding charges (n_c=200). Results for the w_{30} cluster.

Based on x-ray emission spectra and Hartree-Fock calculations for liquid structures generated by molecular dynamics simulations, Guo *et al.*[37] suggested that the strong involvement of the $3a_1$ valence orbitals in H bonding leads to the broadening of $3a_1$ and $1b_2$ bands from the water monomer to small water clusters.[37] The same behavior of the DOS for free water clusters is presently observed. However, by adding embedding charges, a shoulder at ~ -14 eV, which can be associated to the $3a_1$ band, is observed. In addition, the charges contribute to decrease the mixing of $1b_2$ and $3a_1$ bands. This seems to reflect a significant polarization of the $3a_1$ orbital of the water molecules by the charges. We note that polarization of the $3a_1$ orbital was recently invoked to explain the large increase in the water dipole moment upon condensation.[37] Similar changes are also observed when the aggregates are embedded in a dielectric medium, strongly indicating that the mixing of the $3a_1$ and $1b_2$ bands in the water DOS is mainly related to surface effects. However, it should be observed that in contrast with the continuum dielectric method, thermal fluctuactions related to different charge configurations will characterize long-ranged corrections and thermal broadening in the present approach.

In keeping with the behavior for free water clusters of increasing size, the $1b_1$ conduction band is shifted to lower energies, which indicates that the changes on the DOS for occupied orbitals are similar when the cluster size increases or when an embedding charge distribution is added.

When the clusters are embedded by a charge distribution, the DOS of unoccupied orbitals is also modified. First, the DOS associated with the bottom of the conduction band is slightly shifted to higher energies. Second, the peak of the broad distribution related to the $2b_1$ and Rydberg states increases. The first modification is also illustrated in Fig. 6, where the energies of the HOMO and LUMO, as well as E_G are shown as a function of N (the number of uncorrelated MC configurations) for the w_{30} aggregate with and without embedding charges. By adding charges, the LUMO energy is also shifted upwards. This tendency is opposite to what is observed when the cluster size increases. We note that the LUMO energy is related to the water electron affinity, or to the energy needed to solvate an electron, which depends on the number of nonbonded hydrogen atoms. Therefore, a possible explanation for the behavior of the LUMO energy is that by introducing embedding charges, we simulate the presence of water molecules and the corresponding increase of H bonds. We have verified that a similar effect is observed when self-consistent reaction-field calculations based on the Kirkwood-Onsager model are carried out.

IV. EXTRAPOLATION TO LIQUID WATER AND COMPARISON WITH EXPERIMENT

A. Binding energies and gas-to-condensed-phase energy shifts

Table II reports the experimental[22] and theoretical KS

TABLE II. Electron binding energies and gas-to-condensed-phase energy shifts (δE) for valence orbitals. The data are in eV. The theoretical results are for the w_{30} cluster.

	Expt.			Theor.			
Orbital	Gas[a]	Liquid[b]	δE	Free cluster	δE	Embedded cluster	δE
$1b_1$	12.60	11.16±0.04	1.44	11.57±0.18	1.03(1.05)[c]	11.74±0.02	0.86
$3a_1$	14.80	13.50±0.10	1.30	13.83±0.42	0.97(1.12)[c]	14.10±0.03	0.70
$1b_2$	18.60	17.34±0.04	1.26	17.89±0.05	0.71(1.00)[c]	17.69±0.01	0.91
$2a_1$	32.60	30.90±0.06	1.70	33.16±0.02	−0.56	33.04±0.01	−0.44

[a]Electron binding energies for the water monomer. From Banna *et al.* (Ref. 80).
[b]From Winter *et al.* (Ref. 22).
[c]Experimental results for a cluster with $\langle n \rangle$=250 water molecules. From Björneholm *et al.* (Ref. 21).

TABLE III. HOMO-LUMO gap ($E_{G,n}$) and average LUMO energy ($V_{0,n}$) for water clusters. The results are in eV.

	Free clusters		Embedded clusters	
n	$E_{G,n}$	$V_{0,n}$	$E_{G,n}$	$V_{0,n}$
1	12.31	0.35	12.56±0.08	0.68±0.08
2	11.05±0.04	0.03±0.01	11.97±0.08	0.51±0.08
4	10.60±0.03	−0.19±0.03	11.58±0.08	0.34±0.08
8	9.90±0.16	−0.49±0.05	11.25±0.06	0.19±0.07
10	9.50±0.19	−0.66±0.14	11.10±0.05	0.14±0.07
15	9.15±0.25	−0.85±0.14	10.90±0.04	0.04±0.05
20	8.84±0.27	−0.96±0.18	10.71±0.04	−0.02±0.03
30	8.69±0.25	−1.00±0.18	10.48±0.04	−0.15±0.04
⋮				
∞[a]	8.55±0.08	−1.06±0.03	10.41±0.09	−0.17±0.05

[a]Extrapolated values.

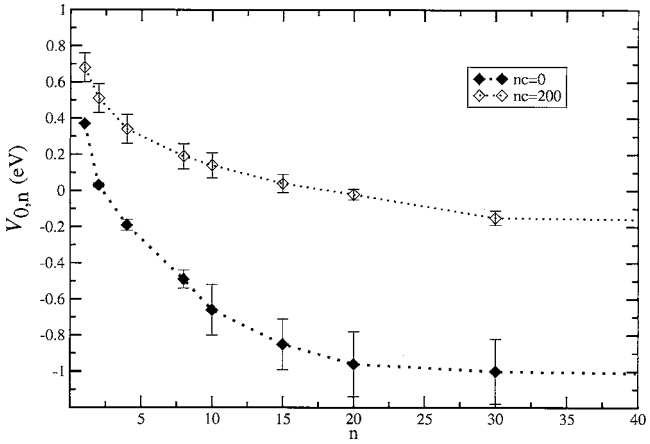

FIG. 7. Size dependence of $V_{0,n}$ for free and embedded water clusters.

electron binding energies, and the gas-to-condensed-phase energy shift (δE) for the valence orbitals. Theoretical values were derived from Gaussian fitting of the DOS, and δE for each orbital is defined as the difference between the experimental electron binding energy for the isolated water molecule[80] and its value in the condensed phase. Theoretical results are for the w_{30} cluster. With the exception of the $2a_1$ orbital, a good agreement between experimental binding energies for liquid water and theoretical results is observed. For the $1b_1$ and $3a_1$ orbitals, experimental binding energies are in better agreement with theoretical results for free water clusters, although the differences are quite small. More important, the redshift of δE, which is a condensed-phase effect, is qualitatively in keeping with experimental information: We find that δE is ~0.9 and 0.7 eV for the $1b_1$ and $3a_1$ orbitals, respectively. The experimental values are ~1.3 eV. The only significant discrepancy relative to experiment concerns the $2a_1$ orbital for which theoretical calculations predict a small blueshift (~0.4 eV), whereas a 1.7-eV redshift is predicted by experiment. Results for free water clusters can be compared with photoemission spectra of water clusters.[21] A good agreement between theoretical and experimental results for the binding energy shift from the molecule to the cluster can be observed, particularly for the $1b_1$ and $3a_1$ orbitals (see Table II).

B. The water electron affinity V_0

V_0 can be defined as the energy to take a zero kinetic-energy gas-phase electron to the bottom of the conduction band of the condensed phase as a delocalized or quasifree electron.[3,18] Several theoretical[23,25] and experimental[3,14] estimates of V_0 were reported. The typical literature value is −1.2 eV.[14] A significantly smaller estimate (−0.12 eV) has been reported.[3] This value is closer to a theoretical prediction by Jortner ($-0.5 < V_0 < 1.0$),[23] and in good agreement with the Henglein's calculation (−0.2 eV).[25]

In the present work $V_{0,n}$ (see Table III) represents V_0 for a cluster with n water molecules. It was estimated as the average LUMO energy of the aggregate. The behavior of $V_{0,n}$ with the number of water molecules (n) is illustrated in Fig. 7. In free water clusters $V_{0,n}$ changes from 0.03 ± 0.01 ($n=2$) to -1.0 ± 0.18 eV ($n=30$). When the electrostatic field of the embedding charges is introduced, significant differences relative to free clusters are observed. In these clusters, $V_{0,n}$ changes from 0.51 ± 0.08 ($n=2$) to -0.15 ± 0.04 eV ($n=30$). It should be expected that non-H-bonded hydrogen atoms at the cluster surface contribute to increase the electron affinity or to lower the LUMO energy. Embedding charges reduce surface effects by simulating the presence of water molecules at the cluster surface and contribute to increase the LUMO energy. Extrapolation of $V_{0,n}$ for $n=\infty$ leads to $V_{0,\infty}=-1.06\pm0.03$ eV (free cluster) and $V_{0,\infty}=-0.17\pm0.05$ eV (embedded cluster). It seems reasonable to assume that the extrapolated average LUMO energy for the embedded water clusters ($V_{0,\infty}$) is a reasonable estimate of the bulk water V_0. Therefore, our result for $V_{0,\infty}$ is in very good agreement with the recent estimate by Coe *et al.*[3] (−0.12 eV) and Henglein[25] (−0.2 eV) but significantly smaller than the value reported by Grand *et al.* (−1.2±0.1 eV).[14]

C. The HOMO-LUMO gap

The HOMO-LUMO gap ($E_{G,n}$) for water clusters of size n is reported in Table III. The values correspond to averages over 50 uncorrelated configurations. The behavior of the average optical gap ($E_{G,n}=\epsilon_{HOMO}-\epsilon_{LUMO}$) with the number of water molecules (n) for free and embedded clusters ($n_c=200$) is illustrated in Fig. 8. In free clusters $E_{G,n}$ changes from 11.05 ± 0.04 ($n=2$) to 8.69 ± 0.25 eV ($n=30$). When embedding charges are introduced $E_{G,n}$ changes from 11.97 ± 0.08 ($n=2$) to 10.48 ± 0.04 eV ($n=30$), indicating a weaker dependence with n in comparison with free clusters. Extrapolated values for the HOMO-LUMO gap ($E_{G,\infty}$) are 8.55 ± 0.08 (free cluster) and 10.41 ± 0.09 eV (embedded cluster). Theoretical informations on the HOMO-LUMO gap of liquid water are relatively scarce. First-principles molecular dynamics of Boero *et al.*[32] estimate the KS HOMO-LUMO gap of liquid water at normal conditions as ~3.6 eV. A previous estimate of 4.65 eV was reported by Laasonen *et al.*[27] The disagreement with the present values illustrates that widely used approximations in density-functional theory lead to gaps that are significantly underestimated. From the theoretical values of $E_{G,\infty}$ and $V_{0,\infty}$ we can estimate the photo-

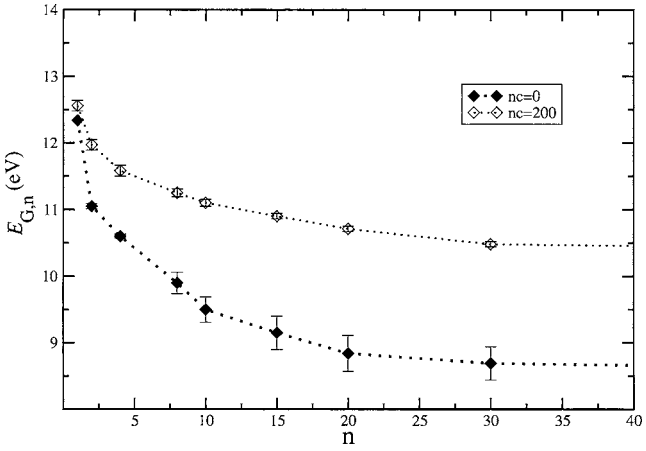

FIG. 8. Size dependence of $E_{G,n}$ for free and embedded water clusters.

electron threshold (PET), which is defined as[17] PET$=E_G+|V_0|$. For free water clusters we find that PET $=9.61\pm0.15$ eV. For embedded water clusters, our extrapolated $E_{G,\infty}$ and $V_{0,\infty}$ leads to PET$=10.58\pm0.10$ eV, which is $\sim$0.5 eV above the experimental values reported by Delahey and Von Burg[15] (10.06 eV) and by Winter *et al.* (9.9 eV).[22] Our theoretical PET is, however, close to an experimental value of $\sim10.5\pm0.5$ eV.[12]

D. The adiabatic band gap of liquid water

The adiabatic band gap of liquid water can be estimated through a thermochemical cycle, which involves several species including H_2O^+, H_3O^+, OH^-, and $OH^\bullet$, and the hydrated electron e^- (aq). A detailed description can be found in Refs. 3 and 4. However, the process can be summarized as follows. Vertical photoionization of liquid water produces an excited H_2O^+ ion and a delocalized e^-(aq). The H_2O^+ formed by ionization reacts quickly by proton transfer to a nearby water molecule leading to the formation of H_3O^+ and of the hydroxide defect OH^-, which can be placed at $\Delta E=0.58$ eV above the valence-band edge. ΔE is the energy of the reaction

$$2H_2O(1) \rightarrow H_3O^+(aq) + OH^-(aq). \quad (2)$$

The conduction-band edge can be associated with

$$H_3O^+(aq) + OH^\bullet(aq) + e^-(cond), \quad (3)$$

where it is assumed that the reorganization of water molecules takes place around the H_3O^+ and $OH^\bullet$ species. By defining a thermochemical cycle[3,4] it is then possible to calculate the water adiabatic band gap by using

$$E_{G,Ad} = \Delta E_{hyd}(OH^\bullet) + V_0 + AEA[OH^\bullet(g)] - \Delta E_{hyd}(OH^-) + \Delta E, \quad (4)$$

where AEA$[OH^\bullet(g)]=1.83$ eV (Ref. 3) is the gas-phase adiabatic electron affinity (AEA) of the OH radical and $\Delta E_{hyd}(OH^-)=-4.97$ eV is the hydration energy of OH^-.[3] The less well-known quantities for predicting $E_{G,Ad}$ are the hydration energy of the OH radical, $\Delta E_{hyd}(OH^\bullet)$, and the water electron affinity V_0. Different works[3,81,82] predicted that $\Delta E_{hyd}(OH^\bullet)$ is close to -0.37 eV. Several electronic properties of liquid water are gathered in Table IV. Based on the Monte Carlo result for $\Delta E_{hyd}(OH^\bullet)=-0.38$ eV (Ref. 82) and the present estimate of V_0, we find that $E_{G,Ad}=6.83\pm0.05$ eV, which is in excellent agreement with the value reported by Coe and co-workers.[3,4]

TABLE IV. Band gap of liquid water. Theoretical and experimental data (in eV).

	This work	Coe *et al.*[a]	Other
$\Delta_{hyd}H(OH^\bullet)$		-0.37	-0.38;[b] -0.37[c]
V_0	-0.17 ± 0.05	-0.12	-1.2 ± 0.1;[d] -0.2[e]
E_G (Theor.)	10.41 ± 0.09		7.8;[f] $\sim3.6\pm0.2$;[g] 4.6 ± 0.05[h]
E_G (Expt.)			7.0;[i] 8.9;[d] 8.7 ± 0.5[j]
$E_{G,Ad}$	6.83 ± 0.05	6.89	
PET	10.58 ± 0.1		10.06;[k] 9.9;[l] 10.5;[m]

[a]From Coe *et al.* (Ref. 3).
[b]From Cabral do Couto *et al.* (Ref. 82).
[c]From Autrey *et al.* (Ref. 81).
[d]From Grand *et al.* (Ref. 14).
[e]From Henglein (Ref. 25).
[f]Band gap for cubic ice. From Parravicini and Resta (Ref. 24).
[g]From Boero *et al.* (Ref. 32).
[h]From Laasonen *et al.* (Ref. 27).
[i]From Goulet *et al.* (Ref. 17).
[j]From Bernas *et al.* (Ref. 19).
[k]From Delahey and Von Burg (Ref. 15).
[l]From Winter *et al.* (Ref. 22).
[m]From Shibaguchi *et al.* (Ref. 12).

V. CONCLUSIONS

Electronic properties of water clusters and liquid water were investigated by sequential Monte Carlo/density-functional theory calculations. DFT calculations were based on the reparametrization of the MPW1PW91 functional that predicts the structural, energetic, and electronic properties of the water dimer in excellent agreement with experimental information. A detailed analysis of the the KS density of states (DOS) and the band gap of water clusters was carried out. Special emphasis was placed on the dependence of the results on the cluster size and surface effects. The behavior of the water DOS with the number of particles and its dependence on surface effects is in keeping with information from x-ray emission and absorption spectra. One relevant conclusion concerns surface effects on the electronic structure of water clusters. It was found that they significantly contribute to the broadening of the water $3a_1$ and $1b_1$ bands that characterize the DOS of water clusters. In addition, surface effects contribute to lower the average LUMO energy in comparison with clusters embedded by a charge distribution, which mimics the presence of water molecules. When the results are extrapolated for larger aggregates embedded in a charge distribution, the results for the water electron affinity (V_0) is in very good agreement with the estimate by Coe *et al.*,[3] and other theoretical calculations. As expected, there is a significant difference between the adiabatic and vertical (HOMO-LUMO) band gap of water. Our result for the adiabatic band gap of liquid water is in excellent agreement with recent predictions.[3,4] The present reparametrization of the MPW1PW91 functional provided reliable information on the

electronic properties of liquid water and indicates that our approach can be of interest for investigating electronic properties of liquids.

ACKNOWLEDGMENTS

This work was partially supported by Fundação para a Ciência e a Tecnologia (FCT), Portugal (Grant No. POCTI/43315/QUI/2001). Two of the authors (S.G.E and P.C.C.) gratefully acknowledge the FCT. (Ph.D. Grants SFRH/BD/10200/2002 and SFRH/XXI/BD/6503/2001.)

[1] *Water a Comprehensive Treatise*, edited by F. Franks (Plenum, New York, 1972), Vol. 1; *Water a Comprehensive Treatise* (Plenum, New York, 1973), Vols. 2 and 3; *Water a Comprehensive Treatise* (Plenum, New York, 1975) Vol. 4.
[2] M. C. R. Symons, Acc. Chem. Res. **14**, 179 (1981).
[3] J. V. Coe, A. D. Earhart, M. H. Cohen, G. J. Hoffman, H. W. Sarkas, and K. H. Bowen, J. Chem. Phys. **107**, 6023 (1997).
[4] J. V. Coe, Int. Rev. Phys. Chem. **20**, 33 (2001).
[5] T. Head-Gordon and G. Hura, Chem. Rev. (Washington, D.C.) **102**, 2651 (2002).
[6] B. Guillot, J. Mol. Liq. **101**, 219 (2002).
[7] R. Rey, K. B. Møller, and J. T. Hynes, Chem. Rev. (Washington, D.C.) **104**, 1915 (2004).
[8] G. Franseze and H. E. Stanley, Physica A **314**, 508 (2002).
[9] Y. Q. Tu and A. Laaksonen, Chem. Phys. Lett. **329**, 283 (2000).
[10] K. Coutinho, R. C. Guedes, B. J. Costa Cabral, and S. Canuto, Chem. Phys. Lett. **369**, 345 (2003).
[11] F. Williams, S. P. Varma, and S. Hillenius, J. Chem. Phys. **64**, 1549 (1976).
[12] T. Shibaguchi, H. Onuki, and R. Onaka, J. Phys. Soc. Jpn. **42**, 152 (1977).
[13] B. Baron, D. Hoover, and F. Williams, J. Chem. Phys. **68**, 1997 (1978).
[14] D. Grand, A. Bernas, and E. Amouyal, Chem. Phys. **44**, 73 (1979).
[15] P. Delahey and K. Von Burg, Chem. Phys. Lett. **83**, 250 (1981).
[16] T. Goulet and J.-P. Jay-Gerin, J. Phys. Chem. **93**, 7532 (1989).
[17] T. Goulet, A. Bernas, C. Ferradini, and J.-P. Jay-Gerin, Chem. Phys. Lett. **170**, 492 (1990).
[18] P. Han and D. M. Bartels, J. Phys. Chem. **94**, 5824 (1990).
[19] A. Bernas, C. Ferradini, and J.-P. Jay-Gerin, Chem. Phys. **222**, 151 (1997).
[20] A. Bernas, C. Ferradini, and J.-P. Jay-Gerin, J. Photochem. Photobiol., A **117**, 171 (1998).
[21] O. Björneholm, F. Federman, S. Kakar, and T. Möller, J. Chem. Phys. **111**, 546 (1999).
[22] B. Winter, R. Weber, W. Widdra, M. Dittmar, M. Faubel, and I. Hertel, J. Phys. Chem. A **108**, 2625 (2004).
[23] J. Jortner, Ber. Bunsenges. Phys. Chem. **75**, 696 (1971).
[24] G. P. Parravicini and L. Resca, Phys. Rev. B **8**, 3009 (1973).
[25] A. Henglein, Can. J. Chem. **55**, 2112 (1977).
[26] P. Cabral do Couto, R. C. Guedes, and B. J. Costa Cabral, Braz. J. Phys. **34**, 42 (2004).
[27] K. Laasonen, M. Sprik, M. Parrinello, and R. Car, J. Chem. Phys. **99**, 9080 (1993).
[28] M. Sprik, J. Hutter, and M. Parrinello, J. Chem. Phys. **105**, 1142 (1996).
[29] P. L. Silvestrelli and M. Parrinello, Phys. Rev. Lett. **82**, 5415 (1999).
[30] P. L. Silvestrelli and M. Parrinello, J. Chem. Phys. **111**, 3572 (1999).
[31] M. Boero, K. Terakura, T. Ikeshoji, C. C. Liew, and M. Parrinello, Phys. Rev. Lett. **85**, 3245 (2000).
[32] M. Boero, K. Terakura, T. Ikeshoji, C. C. Liew, and M. Parrinello, J. Chem. Phys. **115**, 2219 (2001).
[33] P. Hunt, M. Sprik, and R. Vuilleumier, Chem. Phys. Lett. **376**, 68 (2003).
[34] J. VandeVondele, F. Mohamed, M. Krack, J. Hutter, M. Sprik, and M. Parrinello, J. Chem. Phys. **122**, 014515 (2005).
[35] K. R. Wilson, M. Cavalleri, B. S. Rude *et al.*, J. Phys.: Condens. Matter **14**, L221 (2002).
[36] S. Myneni, Y. Luo, L. Å. Näslund *et al.*, J. Phys.: Condens. Matter **14**, L213 (2002).
[37] J.-H. Guo, Y. Luo, A. Augustsson, J.-E. Rubensson, C. Säthe, H. Ågren, H. Siegbahn, and J. Nordgren, Phys. Rev. Lett. **89**, 137402 (2002).
[38] M. Cavalleri, H. Ogasawara, L. G. M. Pettersson, and A. Nilsson, Chem. Phys. Lett. **364**, 363 (2002).
[39] B. Hetényi, F. De Angelis, P. Gianozzi, and R. Car, J. Chem. Phys. **120**, 8632 (2004).
[40] S. Kashtanov, A. Augustsson, Y. Luo *et al.*, Phys. Rev. B **69**, 024201 (2004).
[41] S. Canuto and K. Coutinho, Adv. Quantum Chem. **28**, 89 (1997).
[42] K. Coutinho and S. Canuto, J. Chem. Phys. **113**, 9132 (2000).
[43] C. Adamo and V. Barone, Chem. Phys. Lett. **274**, 242 (1997).
[44] C. Adamo and V. Barone, J. Comput. Chem. **19**, 418 (1998).
[45] C. Adamo and V. Barone, J. Chem. Phys. **108**, 664 (1998).
[46] M. W. Mahoney and W. L. Jorgensen, J. Chem. Phys. **112**, 8910 (2000).
[47] D. Frenkel and B. Smit, *Understanding Molecular Simulation* (Academic, San Diego, 1996).
[48] N. Metropolis, A. W. Rosenbluth, M. N. Rosenbluth, A. H. Teller, and E. Teller, J. Chem. Phys. **21**, 1087 (1953).
[49] J. G. Kirkwood, J. Chem. Phys. **2**, 351 (1934); L. Onsager, J. Am. Chem. Soc. **58**, 1486 (1936).
[50] L. Kleinman, Phys. Rev. B **56**, 16029 (1997).
[51] J. P. Perdew and M. Levy, Phys. Rev. B **56**, 16021 (1997).
[52] X. Hua, X. Chen, and W. A. Goddard III, Phys. Rev. B **55**, 16103 (1997).
[53] P. Politzer and F. Abu-Awwad, Mol. Phys. **95**, 681 (1998).
[54] P. Politzer and F. Abu-Awwad, Theor. Chem. Acc. **99**, 83 (1998).
[55] R. Stowasser and R. Hoffmann, J. Am. Chem. Soc. **121**, 3414 (1999).
[56] F. R. Manby and P. J. Knowles, J. Chem. Phys. **112**, 7002 (2000).
[57] F. Abu-Awwad and P. Politzer, J. Comput. Chem. **21**, 227 (2000).
[58] S. Hamel, P. Duffy, M. E. Casida, and D. R. Salahub, J. Electron Spectrosc. Relat. Phenom. **123**, 345 (2002).
[59] D. P. Chong, O. V. Gritsenko, and E. J. Baerends, J. Chem. Phys. **116**, 1760 (2002).
[60] C.-G. Zhan, J. A. Nichols, and D. A. Dixon, J. Phys. Chem. A **107**, 4184 (2003).
[61] J. Jellinek and P. H. Acioli, J. Chem. Phys. **118**, 7783 (2003).
[62] I. Ciofini, C. Adamo, and H. Chermette, Chem. Phys. **309**, 67 (2005).
[63] C. Y. Ng, D. J. Trevor, P. W. Tiedemann, S. T. Ceyer, P. L. Kronebusch, B. H. Mahan, and Y. T. Lee, J. Chem. Phys. **67**, 4235 (1977).
[64] D. E. Woon and T. H. Dunning, Jr., J. Chem. Phys. **98**, 1358 (1993).
[65] J. Cizek, Adv. Chem. Phys. **14**, 35 (1969).
[66] G. D. Purvis and R. J. Bartlett, J. Chem. Phys. **76**, 1910 (1982).
[67] G. E. Scuseria, C. L. Janssen, and H. F. Schaefer III, J. Chem. Phys. **72**, 4244 (1980).
[68] G. E. Scuseria and H. F. Schaefer III, J. Chem. Phys. **90**, 3700 (1989).
[69] C. Møller and M. S. Pleset, Phys. Rev. **46**, 618 (1934).
[70] V. C. Felic'issimo, I. Minkov, F. F. Guimarães, F. Gel'mukhanov, A. Cesar, and H. Ägren, Chem. Phys. **312**, 311 (2005).
[71] J. A. Odutola and T. R. Dyke, J. Chem. Phys. **75**, 5062 (1980).
[72] M. M. Feyerisen, D. Feller, and D. A. Dixon, J. Phys. Chem. **100**, 2993 (1996).
[73] T. R. Dyke, K. M. Mack, and J. S. Muenter, J. Chem. Phys. **66**, 498 (1977).
[74] J. Kim, I. Becker, O. Cheshnovsky, and M. A. Johnson, Chem. Phys. Lett. **297**, 90 (1998).
[75] Z. S. Huang and R. E. Miller, J. Chem. Phys. **91**, 6613 (1989).
[76] M. J. Frisch, G. W. Trucks, H. B. Schlegel *et al.*, GAUSSIAN-98, Gaussian Inc., Pittsburgh, PA, 1998.
[77] D. M. Chipman, J. Phys. Chem. **83**, 1657 (1979).
[78] K. D. Jordan and F. Wang, Annu. Rev. Phys. Chem. **54**, 367 (2003).
[79] P. F. Flükiger, thèse 2561, Département de Chimie Physique, Université de Genève, Genève, 1992; S. Portmann and H. P. Lüthi, Chimia **54**, 766 (2000).
[80] M. S. Banna, B. H. McQuaide, R. Malutzki, and V. Schmidt, J. Chem. Phys. **84**, 4739 (1986).
[81] T. Autrey, A. K. Brown, D. M. Camaioni, M. Dupuis, N. S. Foster, and A. Getty, J. Am. Chem. Soc. **126**, 3680 (2004).
[82] P. Cabral do Couto, R. C. Guedes, B. J. Costa Cabral, and J. A. Martinho Simões, J. Chem. Phys. **119**, 7344 (2003).